Hindawi
Journal of Nanomaterials
Volume 2019, Article ID 8263843, 9 pages
https://doi.org/10.1155/2019/8263843

Research Article

Directional Gradientless Thermoexcited Rotating System Based on Carbon Nanotubes and Graphene

Xin Wu and Qiang Han

Department of Engineering Mechanics, School of Civil Engineering and Transportation, South China University of Technology, Guangzhou, Guangdong Province 510640, China

Correspondence should be addressed to Qiang Han; emqhan@scut.edu.cn

Received 6 August 2019; Accepted 3 December 2019; Published 20 December 2019

Academic Editor: Michele Zappalorto

The simple and practicable intrinsic driving mechanism is of great significance for the design and development of nanoscale devices. This paper proposes a nanosystem that can achieve directional gradientless thermoexcited rotation at a relatively high temperature field (such as 300 K). In the case of a constant temperature field, the difference in atomic van der Waals (VDW) potentials in different regions of the rotor can be achieved by an asymmetric design of the structure, which provides torque for the rotation of the rotor. We studied the rotation and driving mechanism of the designed system through molecular dynamics (MD) simulation and discussed the influence of the chiral combination of carbon nanotubes, the chirality of graphene substrate, the length of graphene substrate, and the system temperature on rotation. At the same time, this paper also makes a qualitative analysis of the feasibility of the designed system from the perspective of molecular mechanics combined with energy. This research provides a new idea of nanoscale driving rotation, which has guiding significance for the design and application of related nanodevices in the future.

1. Introduction

In 1991, Iijima [1] discovered the carbon nanotube (CNT). Ultra-high-strength mechanical properties and excellent electrothermal properties make this material stand out and have been widely studied. In particular, multiwalled carbon nanotubes (MWCNTs), represented by double-walled carbon nanotubes (DWCNTs), greatly promote the design and research of nanodevices by virtue of their ultralow interlaminar friction and limited motion combination. These include nanooscillators, nanobearings, nanomotors, and nanoconveyors [2–4].

In a previous experimental study, Barreiro et al. [5] proposed an artificial nanomotor in which the mass cargo attached to the outer tube of the DWCNTs can be rotated or translated along the inner tube. The driving source of this case is the temperature gradient. It is significant and offers possibilities for the actual manufacture of nanomotors. At the same time, Tu and Ou-Yang [6] proved the rationality of molecular motor based on DWCNTs from the theoretical perspective and pointed out that the trajectory of rotor motion is determined by the atomic interaction between inner and outer tubes.

So far, there have been many research results on nanodevices with an external thermal gradient drive. According to reports, Schoen et al. [7] demonstrated that the gold nanoparticles undergo regular thermophoretic motion in carbon nanotubes with temperature gradient by an MD method. In further research, the team explained the cause of the movement of gold nanoparticles from the perspective of phonon scattering and found that the chiral characteristics of carbon nanotubes have an effect on the friction of gold particles during motion [8]. It is reported that Shenai et al. [9] proposed a linear molecular motor driven by the thermal gradient based on the DWCNTs and found that the thermophoretic motion of the outer tube can be partially attributed to the existence of the inner tube's temperature gradient. In another study with a similar

model, Hou et al. [10] pointed out that the thermal driving force received is almost constant when the length of the outer tube is greater than 5 nm. In addition, they also found that the trajectory of the outer tube depends on the chiral combination of carbon nanotubes and the temperature of the system. When the system temperature is higher than the critical temperature, the movement of the outer tube exhibits randomness; on the contrary, the movement of the outer tube is limited to the minimum energy orbit. Santamaria-Holek et al. [11] proposed a mechanical model (Langevin model) based on a coaxial DWCNT temperature gradient drive motor. The model combined the effects of friction, VDW force, thermal force, and noises to discuss the effects of different chiral combinations on external tube motion. Guo et al. [12] further proposed the concept of edge force and pointed out that the edge forces that exist at the ends of the outer tube will also play a certain driving role. Huang and Han [4] proposed a controllable nanoscale rotational actuation system and analyzed that the driving torque is derived from the temperature gradient and the VDW potential difference caused by the carbon nanotube shell structure.

In addition to the study of temperature gradient driving, Bourlon et al. [3] introduced an electrode-driven approach to the fabrication of nanoelectromechanical systems and found lower interlaminar friction of approximately 0.85 MPa. Furthermore, Bailey et al. [13] proposed a new CNT electrode driving mechanism that achieves rotation through the torque generated by the electron flux of the chiral nanotubes.

However, in the absence of an externally gradient driving source such as a temperature gradient, Xu et al. [14] designed a large-scale fluctuation device based on carbon nanotubes. It is found that under the common influence of smooth internal potential surface, low mass, and thermal coupling, the inner capsule tube will fluctuate greatly within a certain temperature range, including translation and rotation. And the higher the ambient temperature, the more intense the thermal motion. Cai et al. [15] proposed a thermoinduced nanorotating motor without temperature gradient with the mechanism of using DWCNTs to lose geometric symmetry in a high temperature field. By designing and comparing the contrast models, they found that the higher ambient temperature, the longer outer tube fixed portion, and the closer tube spacing to the equilibrium distance would cause the inner tube to reach a higher rotational speed. However, it is important that the geometric asymmetry in this high temperature field is spontaneous, that is, random. So, it is impossible to effectively control the direction of rotation of the rotor.

In the study, we designed a gradientless thermoexcited rotating system based on carbon nanotubes and graphene under a constant temperature field. It uses the VDW potential energy asymmetry condition of the rotor to generate the driving force and realizes the rotation with controllable direction. In addition, we also qualitatively analyzed the feasibility of the model from the perspective of molecular mechanics combined with energy.

2. Model and Method

The structure of a single CNT is determined by a pair of chiral parameters (n, m) [16], and its radius is

$$r = \left(\frac{\sqrt{3}d_0}{2\pi}\right)\sqrt{n^2 + nm + m^2}, \tag{1}$$

where d_0 is the length of the C-C bond, about 0.142 nm. In particular, when $n = m$, the CNTs are of an armchair type; when $m = 0$, the CNTs are of a zigzag type; in other cases, they are chiral [16]. DWCNTs are represented by $(n_1, m_1)/(n_2, m_2)$. The former represents the inner tube, and the latter represents the outer tube. For single-layer graphene, there are also two different structures of armchair and zigzag in a specific direction, which correspond to different orientations of hexagonal carbon rings.

We select DWCNTs with a double-zigzag combination of $(15, 0)/(24, 0)$ and a graphene substrate with zigzag-type along the y-axis as an example to illustrate the model designed in this study, as Figure 1 shows. The inner tube's length is set to 3 nm and take two rows of atoms fixed at the edges of the both ends; the outer tube's length is 1 nm, and no fixing measures are taken on it. The graphene substrate is 2 nm in the x direction and 1.5 nm in the y direction. The side of the x-axis negative direction is directly below the axis of the DWCNTs, and the vertical distance from the lowermost portion of the outer tube to the substrate is the equilibrium distance $\sigma = 0.34$ nm. For the graphene, the edge which is below the tubes is free, and the other three sides are edge-fixed. In addition, our models also include the different combinations as $(9, 9)/(14, 14)$, $(9, 0)/(18, 0)$, $(10, 0)/(19, 0)$, and $(19, 0)/(28, 0)$ of the commensurate DWCNTs and a zigzag-type graphene substrate along the y-axis direction. A combination of different components with similar geometric parameters provides a control study to investigate the specific effects of different parameters on the rotating system.

The molecular dynamics simulations in this study are based on the Large-Scale Atomic/Molecular Massively Parallel Simulator (LAMMPS) software package [17]. The most important step in this simulation work is the selection of the potential function, which is used to describe the force field between atoms. Therefore, we utilize the adaptive intermolecular reactive empirical bind order (AIREBO) potential as described by Stuart et al. [18] as

$$U = \frac{1}{2}\sum_i \sum_{j\neq i}\left[U_{ij}^{\mathrm{REBO}} + U_{ij}^{L-J} + \sum_{k\neq i,j}\sum_{l\neq i,j,k} U_{kijl}^{\mathrm{tors}}\right], \tag{2}$$

where the U_{ij}^{REBO} term is the REBO potential [19] to describe covalent bonds, shown as

$$E_{ij}^{\mathrm{REBO}} = V_{ij}^{R}(ij) + b_{ij}V_{ij}^{A}(r_{ij}), \tag{3}$$

where V_{ij}^{R} is a repulsive term, V_{ij}^{A} is an attractive term, and b_{ij} is the environment-dependent bond order term

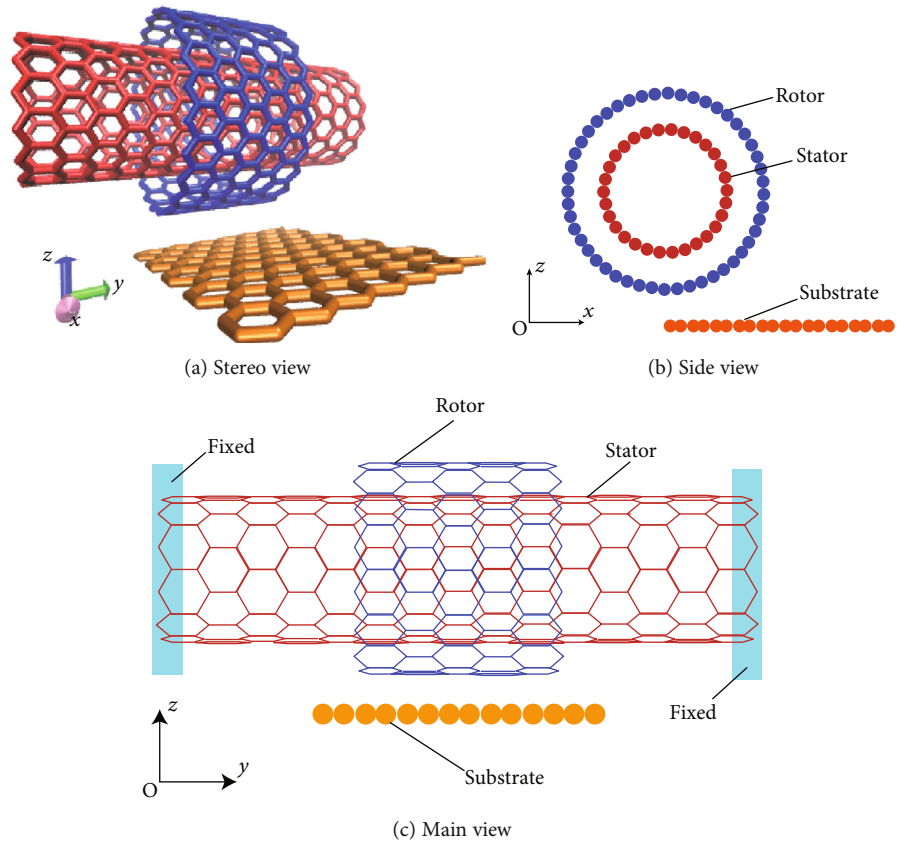

Figure 1: Schematic of the physical model for the nanorotating system.

between atoms, which activates the attractive term only for bonded atoms.

The REBO potential only accounts for interactions of atoms within two angstroms of one another; however, the AIREBO potential also includes the $U_{ij}^{(L-J)}$ term, which is a standard 12-6 Lennard Jones potential. The cutoff for the LJ term is set here to be 2.0 Å as a good balance between computation speed and accuracy. This term is described as

$$U\left(r_{ij}\right) = 4\varepsilon\left[\left(\frac{\sigma}{r_{ij}}\right)^{12} - \left(\frac{\sigma}{r_{ij}}\right)^{6}\right], \tag{4}$$

where r_{ij} represents the distance between atoms, using an equilibrium distance σ of 0.3 4nm and a potential well depth ε value of 2.968 meV in our simulation.

The AIREBO potential also includes the U^{tors} term, which is a four-body potential describing hydrocarbon dihedral angle preference. This potential is best suited for the system of hydrogen and carbon, rendering the all-carbon system well-defined [4, 15]. It is the most suitable one to describe the carbon atom interaction in the rotating nanosystem.

Since this study is a simulation of flexible molecules with variable bond lengths (carbon nanotubes and graphene), the time step was chosen to be 1 fs. The entire simulation process is under the NVT ensemble; that is, the simulated system exchanges energy with the external large heat source to maintain the temperature stability of the analog system. At the same time, the system has a constant volume and atomic number. The movement of the outer tube is limited before each simulation started, and the system is subjected to a 20 ps relaxation at the corresponding temperature using the Nosé-Hoover thermostat. The outer tube is then released, and a molecular dynamics simulation of approximately 8 ns is performed.

3. Results and Discussion

By changing the chirality and size of the components and the ambient temperature of the model, we discuss their effects on the rotating system and analyze the causes of these effects.

3.1. Effect of Different Chiral Combinations of DWCNTs. In order to investigate the effect of different chiral combinations of CNTs on the rotating system, we select a single-layer graphene substrate with a zigzag-type along the y-axis to be in combination with five different CNT models to perform the simulation: $(15, 0)/(24, 0)$, $(9, 9)/(14, 14)$, $(9, 0)/(18, 0)$, $(10, 0)/(19, 0)$, and $(19, 0)/(28, 0)$. The geometric parameters of the various models are shown in Table 1.

First, we select two sets of models (a and b in Table 1) of different chiral combinations and similar geometric parameters for comparative simulation. At the temperature of 300 K, the two rows of atoms at both ends of the stator and the three sides of the substrate are fixed respectively as mentioned

Table 1: Geometric parameters of different chiral combination DWCNTs.

Group	DWCNTs	Chiral combination	Length (nm)	Radius (nm)	Interface radius (nm)	Intertube gap (nm)
a	(15,0)/(24,0)	Zigzag/zigzag	3/1	0.586/0.938	0.762	0.352
b	(9,9)/(14,14)	Armchair/armchair	3/1	0.604/0.948	0.776	0.344
c	(9,0)/(18,0)	Zigzag/zigzag	3/1	0.352/0.704	0.528	0.352
d	(10,0)/(19,0)	Zigzag/zigzag	3/1	0.391/0.743	0.567	0.352
e	(19,0)/(28,0)	Zigzag/zigzag	3/1	0.743/1.095	0.919	0.352

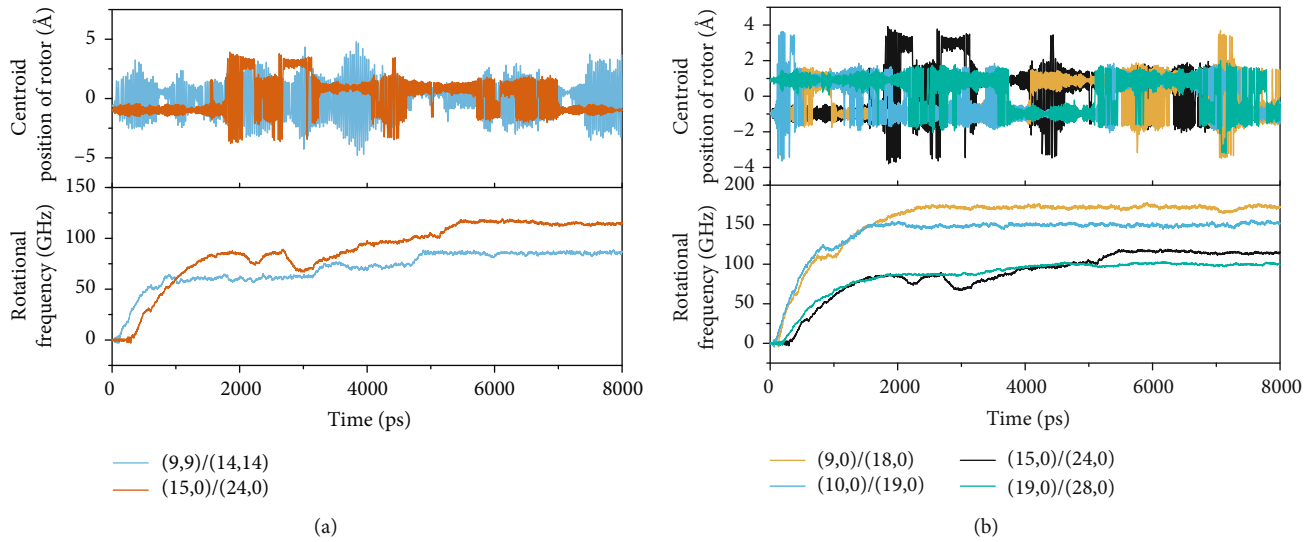

Figure 2: The translation and rotation of the rotor in the systems with different chiral combinations of the DWCNTs: (a) dynamic characteristics of rotors of armchair/armchair and zigzag/zigzag double-tube systems with similar geometric dimensions and (b) dynamic characteristics of the rotors of the zigzag/zigzag chiral combination with different interface radii.

before. The simulation results are shown in Figure 2(a). The upper and lower parts of the figure show the position of the centroid of the rotor and the rotation speed of the rotor as a function of time, respectively. The centroid position of the rotor reflects its translational state, and the lower half shows the rotation speed of the rotor, which reflects the rotational state of the rotor. It can be seen from the graph that with two different chiral combinations, the motion of the rotor is a combined motion of rotation and translation along the axis. The translational motion is an oscillating motion along the axis and is centered on the centroid of the stator. The rotating motion is of variable acceleration, and the speed increases with time and gradually stabilizes. However, it can be clearly seen from the graph that with the chiral combination of (15,0)/(24,0), the rotor can finally obtain a stable rotational frequency of about 114.92 ± 1.41 GHz. In the case of (9,9)/(14,14), the maximum rotational frequency of the rotor is stabilized at around 85.48 ± 1.05 GHz, and more frequent and intense axial oscillations are generated. This is due to the differences in the chiral combination of the two; the zigzag/-zigzag DWCNTs have a potential energy shape that is more prone to relative rotation, whereas the armchair/armchair-type DWCNTs have a potential energy shape that is more prone to relative sliding [20].

Next, we explore the effect of the interface radius [21] on the rotor rotation. The so-called interface radius is the average of the inner and outer carbon nanotube's radii. The same simulations as the above process are performed on the four sets of models numbered a, c, d, and e in Table 1, and the results are shown in Figure 2(b). Among the four sets of simulation results, the radius of the interface is arranged from small to large, and the stable rotational frequencies are 171.552 ± 2.39 GHz, 150.11 ± 2.17 GHz, 114.92 ± 1.41 GHz, and 100.08 ± 1.15 GHz. It is not difficult to find that while the translational states are very similar, the rotor of the system with a smaller interface radius will obtain a relatively larger stable rotational speed. This is because when the interface radius of the double-walled tube system is smaller, the moment of inertia $I = (1/2)mR^2$ is smaller, and a larger proportion of the rotor will be within the range of the VDW force that is from the substrate. For this reason, a double-tube system with a smaller interface radius will eventually achieve a greater stable rotational speed on its rotor.

Therefore, it is not difficult to find from the above analysis that the zigzag/zigzag type of chiral combination and the small interface radius both have a lift on the rotational speed of the rotor.

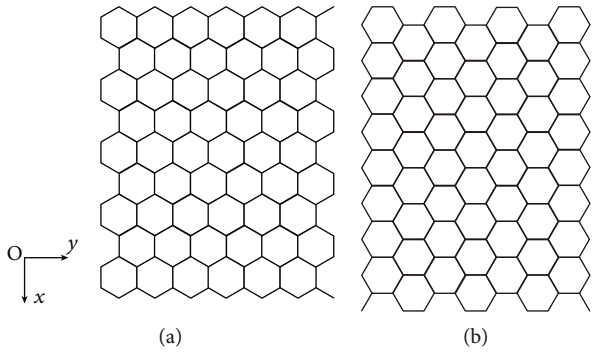

Figure 3: Two graphene substrates of different chiralities along the y-axis with a geometry of 2×1.5 nm: (a) zigzag and (b) armchair.

3.2. Effect of Graphene Substrate Chirality. Due to the difference in arrangement of the hexagonal carbon rings, graphene has two different chiralities—zigzag and armchair—in the same direction (as shown in Figure 3). However, the difference in graphene chirality influences the atomic density of graphene on a specific part and the out-of-plane vibration mode of carbon atoms. In this section, we discuss and study the effects of the graphene substrate's chiral differences.

We select DWCNTs with different chiral combinations (15,0)/(24,0) and (9,9)/(14,14) and build the four different models with the above two chiral graphene substrates. The temperature is 300 K, and the boundary conditions are the same as the previous simulation process; that is, the two ends of the outer tube and the three sides of the base are fixed by two rows of atoms, and the simulation results are shown in Figure 4. As shown in Figure 4(a), for the (15,0)/(24,0) double-tube system, the rotor with the armchair-type graphene substrate has a stable rotation frequency of about 68.07 ± 2.98 GHz, and the stable rotation frequency of the rotor under the action of the zigzag-type graphene substrate can be up to 114.92 ± 1.41 GHz. In another simulation, the final stable rotational frequency of the rotor in the (9,9)/(14,14) double-tube system under the action of the armchair and the zigzag graphene substrate is approximately 57.86 ± 2.24 GHz and 85.48 ± 1.05 GHz, respectively.

The double-tube systems with different chiral combinations and nearly identical sizes show consistent results for the chirality of the graphene substrate to the rotor: in the same case, a zigzag-type graphene substrate along the axial direction of the double-tube system will result in higher rotational speed.

In Figures 3(a) and 3(b), the two graphene substrates (zigzag and armchair, respectively) of the same geometrical size contain 140 and 144 atoms, respectively, and this difference between the two is almost negligible. However, the zigzag-type graphene substrate has a tighter atomic arrangement in the portion near the negative direction of the x-axis; that is, more carbon atoms are closer to the rotor in the rotating system. Therefore, the zigzag-type graphene substrate has a better driving effect, and the rotor in the rotating system using the zigzag-type graphene substrate can obtain a higher rotation speed.

During the process from the start of the simulation to the steady speed, the rotor in the system is driven by the torque from the VDW force of the graphene substrate to rotate. Therefore, we can verify the above-mentioned discussion by calculating and comparing the total torque of the rotor during this process, as shown in Figure 5. The torque (black curve) of the rotor is larger in the case of the two totally different chiral DWCNTs, which are over the zigzag-type graphene. More directly, in the zigzag/zigzag DWCNTs of Figure 5(a), the total torque received by the rotor with the zigzag-type graphene is about 39.5 eV from 0 to 5400 ps, compared with the 17.2 eV of the armchair-type one. The former is almost twice as large as the latter. In the armchair/-armchair double-tube system of Figure 5(b), the total torque received by the rotor with the zigzag and armchair graphene systems is approximately 27.2 eV and 13.7 eV, respectively, from 0 to 5000 ps. The gap between the two is obvious. From this point of view, in the case of the same geometrical size, the use of the zigzag-type graphene as the substrate for the rotating system can greatly improve the rotational speed of the rotor compared with the armchair-type graphene.

3.3. Effect of Graphene Substrate Length. In order to study the effect of the length of the graphene substrate along the y-axis on the rotation, we select the (15,0)/(24,0) DWCNTs and the graphene substrate which is the zigzag-type along the y-axis. The ambient temperature is 300 K. Four sets of simulations with substrate lengths of 1.5 nm, 2.5 nm, 3 nm, and 4 nm in the y-axis direction are performed, respectively, and the length of the substrate varies from approximately the length of the rotor to that of the stator. The boundary setting is the same as before. The simulation results are shown in Figure 6.

In the simulation of four graphene substrate systems with different lengths, the respective rotors are mainly in rotation and translation along the axial direction of the double tubes, and the range of translation is related to the length of the substrate and the stator. When the length of the substrate is smaller than that of the stator, the translation of the rotor exhibits an oscillation motion within the range of the substrate's length; however, when the length of the substrate is greater than that of the stator, the translational range of the rotor depends on the length of the stator. It is not difficult to find from Figure 6 that the system with a graphene substrate which is longer than the rotor will have a large fluctuation or even a decrease in the rotational frequency of the rotor at the end of the simulation. This is because when the length of the substrate is relatively large along the y-axis, it means that the carbon atoms on the graphene will have more severe vibration under thermal motion, which is manifested by a larger amplitude of the substrate carbon atoms along the z-axis. It causes the distance between the substrate carbon atoms and the rotor to be too close at some positions, resulting in a resistance that is opposite to the target torque effect, which ultimately manifests as a weakness on the rotor's rotating speed.

Therefore, in order to ensure that the rotor can obtain a higher stable rotational speed while limiting the axial translation of the rotor, we can select a graphene substrate equivalent to the axial length of the rotor to establish the rotating system.

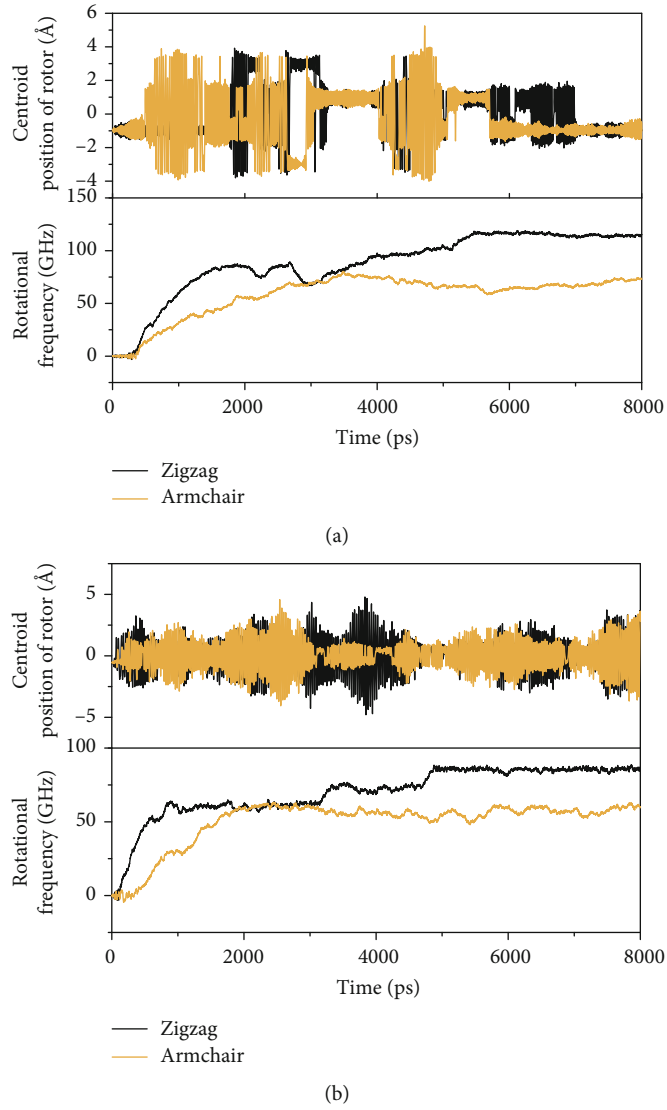

Figure 4: Rotor motion of two different double-tube rotating systems with different chiral graphene substrates: (a) (15.0)/(24,0) and (b) (9,9)/(14,14).

3.4. Effect of Ambient Temperature. In this section, we select (15,0)/(24,0) DWCNTs and zigzag-type graphene substrate models, to perform MD simulation under 20 K, 150 K, 200 K, 250 K, 300 K, 350 K, and 500 K to study the effect of temperature on it. The simulation results are shown in Figure 7. When the ambient temperature is 20 K, the rotor cannot obtain a stable rotation. For the temperature conditions larger than 150 K, the larger the value of the temperature, the greater the final speed that can be obtained by the rotor. At the same time, the higher the ambient temperature, the earlier the rotor can have a certain direction of rotation (from the graph, the earlier it enters the acceleration phase), and the angular acceleration of the rotor acceleration phase is also larger (from the graph, the curve has a larger slope). Specifically, as the ambient temperature increases, the relatively stable rotational frequencies of the respective rotors in the seven different cases are approximately 0.002 ± 1.67 GHz, 65.45 ± 3.34 GHz, 72.53 ± 0.92 GHz, 99.93 ± 1.84 GHz, 114.92 ± 1.41 GHz, 118.21 ± 1.31 GHz, and 151.17 ± 1.82 GHz.

According to statistical thermodynamics,

$$K_{\mathrm{E}} = \sum_{i=1}^{N} \frac{1}{2} m_i v_i^2 = \frac{3}{2} N k_{\mathrm{B}} T_c, \tag{5}$$

where K_{E} is the kinetic energy, N is the total number of atoms in the system, m_i is the mass of the atom i, v_i is the velocity of the atom i, k_{B} is Boltzmann constant, and T_c is the ambient temperature.

Therefore, the thermal motion of carbon atoms will be more intense at higher ambient temperature, which corresponds to the greater velocity of the carbon atoms in the system, which is the cause of the rotor's higher rotational speed. However, high ambient temperature will cause the atomic out-of-plane vibration of the free part of the graphene

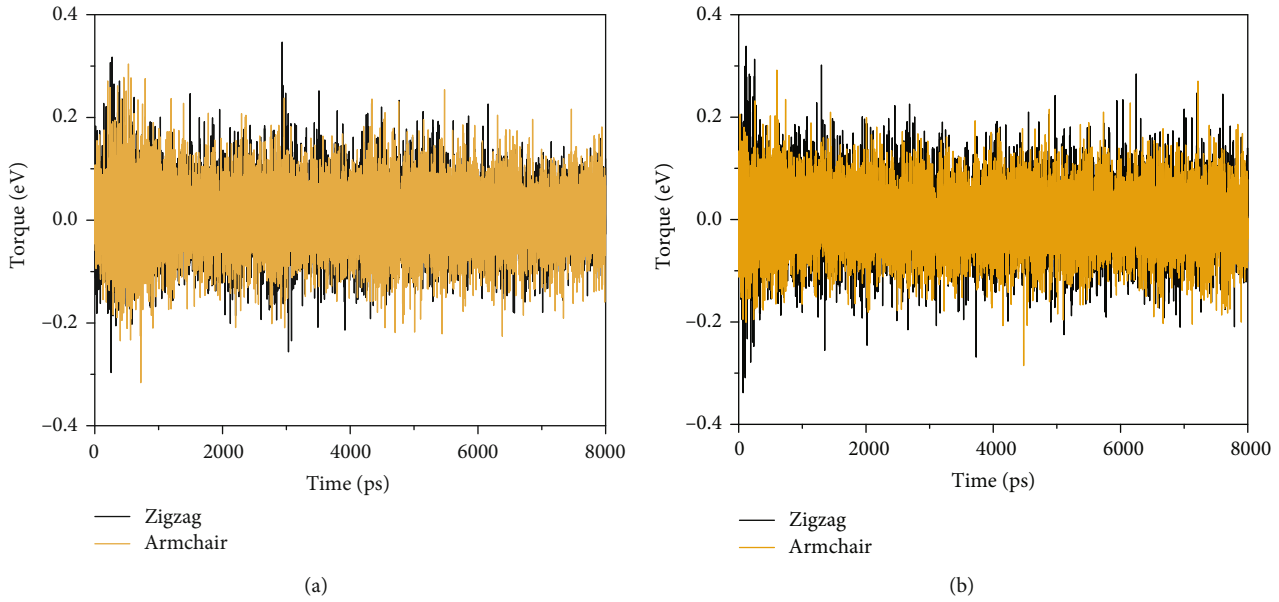

Figure 5: Rotor motion of two different double-tube rotating systems with different chiral graphene substrates: (a) (15.0)/(24,0) and (b) (9,9)/(14,14).

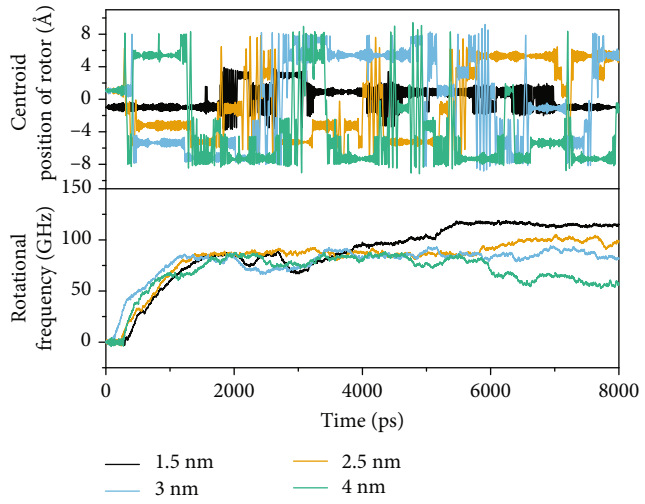

Figure 6: Rotor motion in a rotating system with different lengths of graphene substrate.

substrate to be extremely severe. To a certain extent, this may cause energy dissipation to reduce the rotational efficiency of the rotor. In the simulation, there may even be cases where the rotor and the substrate carbon atoms are recombined due to the too close distance. Therefore, an ambient temperature around 300 K like room temperature is a good temperature choice for this nanodevice system.

4. Analysis of the Rotation Mechanism

It can be seen from some of the above simulation results that the rotational frequency of the outer tube rotor increases to a certain stable value within the simulation time, which means that the rotor is subjected to the torque driving effect to increase the rotational speed. It also can be analyzed from the rotational frequency curve that the magnitude of the torque is almost constant and the direction is unique. Stemming from the designed model above and considering the asymmetry of its structure, we calculate and compare the potential energy of atoms at different positions on the rotor.

As shown in Figure 8, we take the (15,0)/(24,0) DWCNTs and the zigzag-type graphene substrate model as examples to divide some carbon atoms into groups. Each group consists of a row of 6 carbon atoms along the y-axis at the specific location, and the calculation of the respective potential energy is performed during the 200 ps relaxation period. The final results are shown in Figure 9. With the seventh group of atoms as the boundary, the left and right atoms have an obvious potential energy difference. It is obvious that the peak of potential energy appears at the eighth set of atoms, which is about -41.30 eV instead of the seventh set of atoms. And overall, the total potential energy of the carbon atoms away from the side of the substrate is much smaller than that near the substrate side. According to classical mechanics, the force of any atom in the system is the gradient of potential energy:

$$\vec{F}_\tau = -\nabla_i U = -\left(\vec{i}\,\frac{\partial}{\partial x_i} + \vec{j}\,\frac{\partial}{\partial y_i} + \vec{k}\,\frac{\partial}{\partial z_i}\right) U, \tag{6}$$

where U is the potential energy of the atom.

The force acting on the surface of the rotor in its tangential direction $\vec{F}_\tau$ corresponds to the torque in the clockwise direction:

$$M = \vec{F}_\tau R. \tag{7}$$

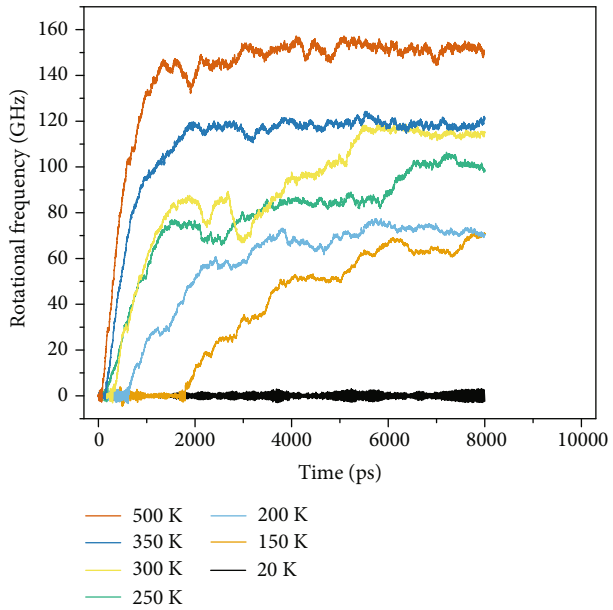

Figure 7: Effect of different ambient temperatures on rotor rotation

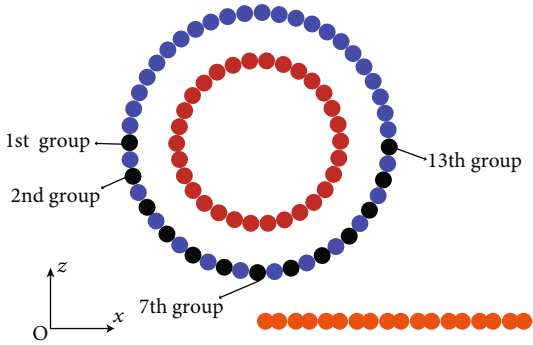

Figure 8: Schematic diagram of carbon atom grouping of the example physical model (the stator atoms are colored in red, the substrate atoms are colored in orange, and the rotor atoms are colored in black and blue, where the black atoms are the atoms in the group).

Under the action of this torque, the rotor overcomes the resistance to obtain the angular acceleration and starts the directional rotation.

According to the above qualitative analysis, we explain the mechanism of the rotating system. However, the rotor speed eventually stabilizes, indicating that the effect of the torque is gradually offset, and eventually the rotor is almost zero in the tangential force. This is because as the rotational speed increases, the friction will increase until it is balanced with the torque so that the tangential force of the rotor in the circumference is zero, and the rotor tends to stabilize at a constant rotational speed [22].

From the perspective of energy sources, the structure of DWCNTs is relatively stable, and regular motion does not occur. However, due to the intervention of the graphene substrate, the initial energy is brought to the whole system,

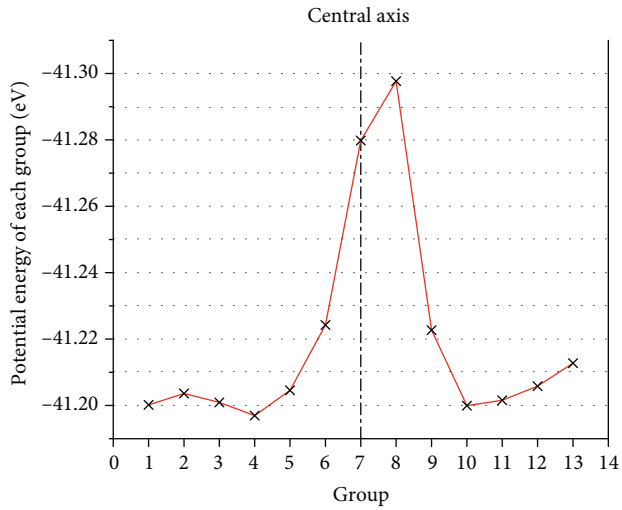

Figure 9: Comparison of the potential energy of each group of atoms in Figure 8

which may be the energy source of the rotor motion. This energy is generally positively correlated with the temperature, and due to some other properties of the structure, the above-described regularity is finally exhibited. Our operations to the entire system, including the intervention of graphene and the setting of boundary conditions, all require energy. Furthermore, the thermal bath conditions in NVT ensemble of MD simulation are accompanied by energy input. Therefore, the "perpetual motion machine" fallacy does not exist with our model.

5. Conclusion

In summary, this paper utilizes the unique physical structure and properties of carbon nanotubes and graphene and designs a directional rotating system based on them under constant temperature field. The feasibility of this model is revealed by MD simulation, molecular mechanics theory, and energy analysis. We considered five factors that may incite the rotor's rotational speed: a zigzag/zigzag DWCNTs with a small interface radius, a zigzag-type graphene substrate with the similar length to the rotor, and a relatively high ambient temperature. By virtue of the asymmetry of the structure itself, the nanorotor thermoexcited rotation with stable speed and controllable direction can be realized without any gradient drive source, which may be helpful for the development of nanodevices in the future.

Data Availability

The simulation data used to support the findings of this study are available from the corresponding author upon request.

Conflicts of Interest

The authors declare that they have no conflicts of interest.

Acknowledgments

The authors are grateful for the support from the National Natural Science Foundation of China (11772130).

References

[1] S. Iijima, "Helical microtubules of graphitic carbon," *Nature*, vol. 354, no. 6348, pp. 56–58, 1991.

[2] Q. Zheng and Q. Jiang, "Multiwalled carbon nanotubes as gigahertz oscillators," *Physical Review Letters*, vol. 88, no. 4, article 045503, 2002.

[3] B. Bourlon, D. C. Glattli, C. Miko, L. Forró, and A. Bachtold, "Carbon nanotube based bearing for rotational motions," *Nano Letters*, vol. 4, no. 4, pp. 709–712, 2004.

[4] J. Huang and Q. Han, "Controllable nanoscale rotating actuator system based on carbon nanotube and graphene," *Nanotechnology*, vol. 27, no. 15, p. 155501, 2016.

[5] A. Barreiro, R. Rurali, E. R. Hernandez et al., "Subnanometer motion of cargoes driven by thermal gradients along carbon nanotubes," *Science*, vol. 320, pp. 775–778, 2008, https://science.sciencemag.org/content/320/5877/775320.

[6] Z. C. Tu and Z. C. Ou-Yang, "A molecular motor constructed from a double-walled carbon nanotube driven by temperature variation," *Journal of Physics: Condensed Matter*, vol. 16, pp. 1287–1292, 2004.

[7] P. A. E. Schoen, J. H. Walther, S. Arcidiacono, D. Poulikakos, and P. Koumoutsakos, "Nanoparticle traffic on helical tracks: thermophoretic mass transport through carbon nanotubes," *Nano Letters*, vol. 6, no. 9, pp. 1910–1917, 2006.

[8] P. A. E. Schoen, J. H. Walther, D. Poulikakos, and P. Koumoutsakos, "Phonon assisted thermophoretic motion of gold nanoparticles inside carbon nanotubes," *Applied Physics Letters*, vol. 90, no. 25, article 253116, 2007.

[9] P. M. Shenai, Z. Xu, and Y. Zhao, "Thermal-gradient-induced interaction energy ramp and actuation of relative axial motion in short-sleeved double-walled carbon nanotubes," *Nanotechnology*, vol. 22, no. 48, p. 485702, 2011, https://iopscience.iop.org/article/10.1088/0957-4484/22/48/22.

[10] Q.-W. Hou, B.-Y. Cao, and Z.-Y. Guo, "Thermal gradient induced actuation in double-walled carbon nanotubes," *Nanotechnology*, vol. 20, no. 49, p. 495503, 2009.

[11] I. Santamaria-Holek, D. Reguera, and J. M. Rubi, "Carbon-nanotube-based motor driven by a thermal gradient," *The Journal of Physical Chemistry C*, vol. 117, no. 6, pp. 3109–3113, 2013.

[12] Z. Guo, T. Chang, X. Guo, and H. Gao, "Mechanics of thermophoretic and thermally induced edge forces in carbon nanotube nanodevices," *Journal of the Mechanics and Physics of Solids*, vol. 60, no. 9, pp. 1676–1687, 2012.

[13] S. W. D. Bailey, I. Amanatidis, and C. J. Lambert, "Carbon nanotube electron windmills: a novel design for nanomotors," *Physical Review Letters*, vol. 100, no. 25, article 256802, 2008.

[14] Z. Xu, Q.-S. Zheng, and G. Chen, "Thermally driven large-amplitude fluctuations in carbon-nanotube-based devices: molecular dynamics simulations," *Physical Review B*, vol. 75, no. 19, article 195445, 2007.

[15] K. Cai, Y. Li, Q. H. Qin, and H. Yin, "Gradientless temperature-driven rotating motor from a double-walled carbon nanotube," *Nanotechnology*, vol. 25, no. 50, p. 505701, 2014.

[16] A. V. Belikov, Y. E. Lozovik, A. G. Nikolaev, and A. M. Popov, "Double-wall nanotubes: classification and barriers to walls relative rotation, sliding and screwlike motion," *Chemical Physics Letters*, vol. 385, no. 1-2, pp. 72–78, 2004.

[17] S. Plimpton, "Fast parallel algorithms for short-range molecular dynamics," *Journal of Computational Physics*, vol. 117, no. 1, pp. 1–19, 1995.

[18] S. J. Stuart, A. B. Tutein, and J. A. Harrison, "A reactive potential for hydrocarbons with intermolecular interactions," *The Journal of Chemical Physics*, vol. 112, no. 14, pp. 6472–6486, 2000.

[19] D. W. Brenner, "Empirical potential for hydrocarbons for use in simulating the chemical vapor deposition of diamond films," *Physical Review B*, vol. 42, no. 15, pp. 9458–9471, 1990.

[20] R. Saito, R. Matsuo, T. Kimura, G. Dresselhaus, and M. S. Dresselhaus, "Anomalous potential barrier of double-wall carbon nanotube," *Chemical Physics Letters*, vol. 348, no. 3-4, pp. 187–193, 2001.

[21] E. H. Cook, M. J. Buehler, and Z. S. Spakovszky, "Mechanism of friction in rotating carbon nanotube bearings," *Journal of the Mechanics and Physics of Solids*, vol. 61, no. 2, pp. 652–673, 2013.

[22] B. E. Zhu, Z. Y. Pan, Y. X. Wang, and Y. Xiao, "Thermal effect on DWCNTs as rotational bearings," *Nanotechnology*, vol. 19, no. 49, p. 495708, 2008.